can be employed to control the formation of two-dimensional features in three-dimensional structures. $Ba_2La_2Cu_2Sn_2O_{11}$ and other multication compounds such as high-temperature superconductors adopt a common and relatively simple structure type (perovskite), but their crystal chemistry is complex and leads to complicated distortions of the basic structure. The nature of the distortions and their effect on the structure and solid-state chemistry must be understood in order to control and ultimately understand their electronic and other physical properties. Superconductivity may be possible in $Ba_2La_2Cu_2Sn_2O_{11}$ provided several factors can be addressed and overcome, such as the inability to chemically oxidize or reduce the compound, the diminished overlap of the copper $d_{x^2-y^2}$ and oxygen 2p orbitals, and the control of the microstructure by thermal or chemical treatments.

Acknowledgment. This work benefitted from the use of the Intense Pulsed Neutron Source at Argonne National Laboratory with funding provided by the National Science Foundation and the Science and Technology Center for Superconductivity (NSF-DMR-8809854). The authors thank R. Hitterman and J. Richardson for their assistance with the neutron diffraction experiment. We gratefully acknowledge J. P. Thiel and J. T. Vaughey for helpful discussions. We also acknowledge the Northwestern Materials Research Center for support of the X-ray Diffraction Facility (MRL-DMR-8821571).

Registry No. $Ba_2La_2Cu_2Sn_2O_{11}$, 144224-60-2.

High-Temperature Chemistry of the Conversion of Siloxanes to Silicon Carbide

Gary T. Burns,† Richard B. Taylor,† Youren Xu,‡ Avigdor Zangvil,‡ and Gregg A. Zank*,†

Dow Corning Corporation, Midland, Michigan 48686-0995, and Materials Research Laboratory, University of Illinois at Urbana—Champaign, Urbana, Illinois 61801

Received June 12, 1992. Revised Manuscript Received August 7, 1992

The preparation of siloxane polymers as precursors to silicon carbide has been investigated. To make these polymers useful as binder materials for ceramic powders in the preparation of dense (sintered) ceramic monoliths, methods were developed to control the silicon carbide to carbon ratios in the polymer derived ceramic. Insights into the chemistry of the conversion of these high oxygen polymers to silicon carbide ceramics were obtained by following the pyrolysis products by elemental analysis, quantitative X-ray diffraction, ^{29}Si MAS NMR spectroscopy, Raman spectroscopy, and transmission electron microscopy. The pyrolysis proceeds by the formation of an amorphous SiCO material at 1200 °C that continues to undergo an Si–O for Si–C bond redistribution so that trace amounts of β-SiC are seen at 1400 °C. By 1600 °C the carbothermic reduction is well underway with only a small percentage of oxygen remaining in the material. At 1800 °C the pyrolysis is complete. The final ceramic is composed of substantial amounts of crystalline β-SiC and excess carbon that is present as turbostratic graphite.

Introduction

Since the discovery of polycarbosilane by Yajima[1] and its subsequent demonstration as a silicon carbide precursor, a variety of polymeric precursors to silicon carbide have been prepared.[2] While these polymeric precursors represent synthetic accomplishments, they also present a variety of challenges for the polymers to be of true ceramic utility. The majority of these polymers were developed to "simplify" the fabrication of ceramic films, fibers, composites, and monoliths. Currently shaped ceramic parts are made by die pressing, injection, and resin transfer molding, composite reinfiltration and extrusion processes that employ fugitive binders. Unfortunately, few of the published polymeric routes to ceramics have the synthetic versatility to tailor the polymer's rheology, cure chemistry, and ceramic composition to the fabrication process required to make a ceramic article.

Within our laboratories we have been investigating a variety of preceramic polymers that would be suitable as binders for the sintering of SiC powders.[3-5] Since 1953 several literature reports have surfaced that detail the requirements for pressureless sintering of SiC monoliths:[6] (1) high-purity submicron spherical powder; (2) the presence of 0.3–2 wt % added carbon; (3) a sintering aid, which is most commonly boron or aluminum; (4) processing to high temperatures, generally above 2000 °C. On the basis of these requirements, we have attempted to prepare polymers that not only function to bind the powders together but also decompose by temperatures of 2000 °C to add sufficient amounts of carbon for densification and additional silicon carbide to reduce the overall shrinkage associated with the sintering process.

Siloxanes and silsesquioxane sol–gels have been prepared and touted as useful in a variety of ceramic applications such as precursors to powders: silicon oxynitride,[7] silicon

† Dow Corning Corp.
‡ University of Illinois.

(1) Yajima, S.; Hayashi, J.; Omori, M. *Chem. Lett.* **1975**, 931.
(2) Baney, R.; Chandra, G. In *Encyclopedia of Polymer Science and Engineering*; John Wiley and Sons: New York, 1988; Vol. 13, pp 312–44.
(3) Burns, G. T.; Saha, C. K.; Zank, G. A.; Freeman, H. A. *J. Mater. Sci.* **1992**, *27*, 2131–40.
(4) Atwell, W. H.; Burns, G. T.; Zank, G. A. In *Inorganic and Organometallic Polymers and Oligomers*; Kluwer Academic Publishers: Dordrecht, The Netherlands, **1990**; pp 147–59.
(5) Taylor, R. B.; Zank, G. A. *Polym. Prepr. (Am. Chem. Soc., Div. Poly Chem.)* **1991**, *32*, 586–7.
(6) (a) Alliegro, R. A.; Tinklepaugh, T. R. *J. Am. Ceram. Soc.* **1953**, *9*, A161. (b) Alliegro, R. A.; Coffin, L. B.; Tinklepaugh, T. R. *J. Am. Ceram. Soc.* **1956**, *12*, 386–9.
(7) Kamiya, K.; Makoto, O.; Yoko, T. *J. Non-Cryst. Solids* **1986**, *83*, 208.

0897-4756/92/2804-1313$03.00/0

oxycarbide,[8] silicon carbide if an additional carbon source is employed,[9] and black glass matrices for composite materials.[10] Since 1987 we have been pursuing similar siloxane polymers as precursors to silicon carbide, that are useful as binders for the sintering of SiC monoliths.[11] The properties of these resins that make them attractive as binders are (1) facile synthesis, (2) thermal and aerobic stability for subsequent processing, (3) compatibility with the ceramic powder, (4) decomposition into stable ceramics comprised *only* of SiC and C at temperatures below those required for the sintering of SiC (~2000 °C), (5) controllable char stoichiometry so that a range of binder levels can be employed while providing sufficient "excess" carbon for sintering,[9,12,13] and (6) a sufficient char yield to minimize the amount of volatiles evolved in the pyrolysis.

The fact that siloxane polymers can be converted into silicon carbide and carbon in controllable amounts makes them useful as binders for the sintering of silicon carbide monoliths. Insights into the pyrolysis chemistry of siloxane materials to 1500 °C are in the literature. In 1987 Fox et al. reported that heating $(PhSiO_{1.5})_x$ gels to 1500 °C produced "a partially crystalline, partially amorphous mixture of β-SiC, SiO_2, and C" as detected by XRD and IR.[8] ^{29}Si MAS NMR evidence for the formation of small amounts of β-SiC from $(Me_2SiO)_x(SiO_2)_{1-x}$ was provided by Babonneau et al.[14] After pyrolysis to 1500 °C the ceramic products from these resins were likewise found to be complex mixtures of SiC, SiO_2, and C as determined by additional IR and XRD analysis of the ceramics.

We have found that simple siloxane polymers are useful as binders for the preparation of sintered SiC monoliths by a variety of processing techniques (die pressing, isopressing, injection molding, extrusion, etc.). Some of the major advantages that these polymer binders bring to sintering SiC over the use of conventional binder systems are (1) a polymeric route to the addition of the required excess carbon needed to limit excessive grain growth, (2) deep section cure that allows for ease of handling and machining in the green state, (3) conversion to SiC which eliminates the need for a binder removal step in the processing and (4) a reduction in the shrinkage associated with the sintering process. In this paper we will discuss the characterization of ceramics derived from a series of siloxane polymers after pyrolysis to temperatures that encompass the carbothermic reduction region of the pyrolysis.

Experimental Procedure

All reactions were carried out in an argon atmosphere in laboratory glassware. All of the siloxane raw materials were obtained from Dow Corning Corp. or were purchased from Hüls Systems. Trifluoromethanesulfonic acid was purchased from Aldrich Chemical Co.

All NMR spectra were recorded on a Varian VXR400S spectrometer. Solution spectra were recorded in $CDCl_3$ in a 5-mm switchable probe (^1H, 399.95 MHz) or a 16-mm Si-free probe (^{29}Si, 79.46 MHz) and referenced to internal $CDCl_3$ (7.25 ppm ^1H) or TMS (0 ppm). The integrals were normalized and calculated relative to the siloxane species. $Cr(acac)_3$ (0.02 M) was added for the ^{29}Si spectra to ensure quantitative acquisition. Solid-state ^{29}Si MAS NMR spectra were acquired with a Jacobsen 7-mm RT CP/MAS probe. The ^{29}Si frequency was 79.459 MHz. Samples were spun at 4 kHz, and the acquisition time was 0.05 s with a 50-kHz spectral window. A 90° pulse width of 10 μs with a relaxation delay of 60 s between pulses was used. Five hundred scans were signal averaged for each sample, zero-filled to 16k data points and processed with 100–300 Hz of Lorentzian line broadening. Chemical shifts were referenced to external TMS.

Gel permeation chromatography (GPC) data were obtained on a Waters GPC equipped with a Model 600E systems controller, Model 490 UV and 410 differential refractometer detector interfaced to a Digital Professional 380 computer employing Waters "Expert" software; all values are relative to polystyrene standards. Thermal gravimetric analyses (TGA) were recorded on an Omnitherm thermal gravimetric analyzer interfaced to an IBM PS/2–50 Z computer with Thermal Sciences software.

Carbon, hydrogen, and nitrogen analyses were done on a Control Equipment Corp. 240-XA elemental analyzer. Oxygen analyses were done on a Leco oxygen analyzer equipped with an Oxygen Determinator 316 (Model 783700) and an Electrode Furnace EF100. Silicon was determined by a fusion technique which consisted of converting the silicon material to soluble forms of silicon and analyzing the solute for total silicon by atomic absorption spectrometry.

All furnace firings were done in an Astro graphite furnace equipped with Eurotherm temperature controllers. The furnace was equipped with an Ircon Modeline Plus optical pyrometer to monitor the temperature above 900 °C.

Samples for quantitative X-ray diffraction analysis (XRD) were prepared by grinding in a B_4C grinder, weighed, and loaded into silicon sample holders. The analysis was carried out on a Norelco Philips vertical goniometer, Model 42271/0 fitted with a closed sample chamber, sample spinner, graphite monochromater, scintillation counter and a long fine-focus Cu target tube. Scans were made at 1°/min from 6 to 80° 2θ with the X-ray operated at 40 kV and 20 mA. The data were analyzed by manual search of the peak intensity and location through standard powder diffraction files.

Raman spectra were recorded on a Nicolet FT-Raman system employing a Nd:YAG laser (1064-nm excitation) at 200-mW laser power. The samples were diluted to 25 wt % in KBr as a pellet. Spectra were obtained by employing 200 scans at a 180° excitation/collection geometry with four Raman wavenumber resolution. The heat emission from the samples was so large that spectra were overwhelmed by heat artifacts from 2000 to 3200 Raman wavenumbers.

Samples for transmission electron microscopy (TEM) were prepared by crushing some of the material and mounting the powder on a copper grid cover ed by a holey carbon film. Samples were studied on Philips Models CM12 and 420 TEMs, the former enabling 0.25-nm resolution (but no microchemical analysis) and the latter having an ultrathin window energy dispersive X-ray analytical capability.

Polymer Synthesis. Employing the following detailed procedure, the polymers described in examples I–XI were prepared:

Example I: $(PhSiO_{1.5})_{0.25}(MeSiO_{1.5})_{0.50}(ViMe_2SiO_{0.5})_{0.25}$. A reaction vessel consisting of a 1-L three-necked flask fitted with a mechanical stirrer, condenser, and a thermometer was charged with 1 g of trifluoromethane sulfonic acid and 100 g of water under an argon atmosphere. A mixture of 74.3 g (0.375 mol) of $PhSi(OMe)_3$, 102 g (0.75 mol) of $MeSi(OMe)_3$, and 34.9 g (0.375 mol) of $(ViMe_2Si)_2O$ was added to the acid water solution resulting in a mild exotherm. After stirring approximately 20 min, the reaction was refluxed for 12 h. After refluxing, the reaction was cooled and the aqueous slurry neutralized with 3.5 g of potassium carbonate. The condenser was removed and replaced with a distillation head and the volatiles (methanol and water) removed by simple distillation until an internal pot temperature of greater than 100 °C was obtained. The reaction mixture was cooled and 205 g of toluene and 20.5 g of a 3 wt % solution of KOH in water added. The distillation head was replaced by a Dean–Stark trap and a condenser and the slurry was refluxed and the water removed through the trap. After all of the water was removed, the

(8) (a) White, D. A.; Oleff, S. M.; Boyer, R. D.; Budinger, P. A.; Fox, J. R. *Adv. Ceram. Mater.* **1987**, *2*, 45–52. (b) White, D. A.; Oleff, S. M.; Fox, J. R. *Adv. Ceram. Mater.* **1987**, *2*, 53–59.

(9) Wei, C. G.; Kennedy, C. R.; Harris, L. A. *Am. Ceram. Soc. Bull.* **1984**, *63*, 1054–61.

(10) (a) Renlund, G. M.; Prochaska, S.; Doremus, R. H. *J. Mater. Res.* **1991**, *6*, 2716–22. (b) Renlund, G. M.; Prochaska, S.; Doremus, R. H. *J. Mater. Res.* **1991**, *6*, 2723–34.

(11) Atwell, W. H.; Burns, G. T.; Saha, C. K. U.S. Patent 4,888,376, 1989.

(12) Negita, K. J. *J. Am. Ceram. Soc.* **1986**, *69*, C308–10.

(13) Antonova, N. D.; Kalinina, A. A.; Kudryavestev, V. I. *Ceram. (Engl. Transl.)* **1962**, *6*, 444–9.

(14) Babonneau, F.; Thorne, K.; Mackenzie, J. D. *Chem. Mater.* **1989**, *1*, 554–8.

Table I. Polymer Synthesis

example	composition	$PhSi(OMe)_3$, g	$MeSi(OMe)_3$, g	$(Me_2ViSi)_2O$, g	yield, g
I	$(PhSiO_{1.5})_{0.25}(MeSiO_{1.5})_{0.50}(Me_2ViSiO_{0.5})_{0.25}$	74.3	102.0	34.9	126 (94.3%)
II	$(PhSiO_{1.5})_{0.30}(MeSiO_{1.5})_{0.45}(Me_2ViSiO_{0.5})_{0.25}$	89.1	91.8	34.9	127 (91.9%)
III	$(PhSiO_{1.5})_{0.35}(MeSiO_{1.5})_{0.40}(Me_2ViSiO_{0.5})_{0.25}$	104.0	81.6	34.9	130 (91.0%)
IV	$(PhSiO_{1.5})_{0.40}(MeSiO_{1.5})_{0.35}(Me_2ViSiO_{0.5})_{0.25}$	467	286	137.5	550 (94.5%)
V	$(PhSiO_{1.5})_{0.45}(MeSiO_{1.5})_{0.30}(Me_2ViSiO_{0.5})_{0.25}$	133.6	61.0	34.9	141 (92.7%)
VI	$(PhSiO_{1.5})_{0.50}(MeSiO_{1.5})_{0.25}(Me_2ViSiO_{0.5})_{0.25}$	148.5	51.0	34.9	145 (92.5%)
VII	$(PhSiO_{1.5})_{0.55}(MeSiO_{1.5})_{0.20}(Me_2ViSiO_{0.5})_{0.25}$	163.35	40.8	34.9	144 (89.2%)
VIII	$(PhSiO_{1.5})_{0.60}(MeSiO_{1.5})_{0.15}(Me_2ViSiO_{0.5})_{0.25}$	178.2	30.6	34.9	157 (94.6%)
IX	$(PhSiO_{1.5})_{0.65}(MeSiO_{1.5})_{0.10}(Me_2ViSiO_{0.5})_{0.25}$	193.0	20.4	34.9	149 (87.3%)
X	$(PhSiO_{1.5})_{0.70}(MeSiO_{1.5})_{0.05}(Me_2ViSiO_{0.5})_{0.25}$	208.0	10.2	34.9	158 (90.1%)
XI	$(PhSiO_{1.5})_{0.75}(Me_2ViSiO_{0.5})_{0.25}$	222.75		34.9	163 (90.6%)

Table II. Polymer Characterization

	GPC			TGA	elem anal. (wt %)				
example	M_n	M_w	M_z	yield[a] (%)	C	H	O	Si	composition as determined by ^1H NMR[b]
I	1999	6824	15974	75.6	40.5	5.43	18.03	31.7	$(PhSiO_{1.5})_{0.24}(MeSiO_{1.5})_{0.48}(Me_2ViSiO_{0.5})_{0.28}$
II	1231	6477	15149	67.8	42.6	5.49	17.68	30.0	$(PhSiO_{1.5})_{0.29}(MeSiO_{1.5})_{0.45}(Me_2ViSiO_{0.5})_{0.26}$
III	1322	5936	13601	72.8	44.0	5.33	17.52	28.7	$(PhSiO_{1.5})_{0.32}(MeSiO_{1.5})_{0.42}(Me_2ViSiO_{0.5})_{0.26}$
IV	1209	4456	63827	67.6	46.5	5.50	17.52	28.6	$(PhSiO_{1.5})_{0.40}(MeSiO_{1.5})_{0.39}(Me_2ViSiO_{0.5})_{0.21}$
V	1822	11143	98730	70.3	48.0	5.60	16.41	31.5	$(PhSiO_{1.5})_{0.45}(MeSiO_{1.5})_{0.30}(Me_2ViSiO_{0.5})_{0.25}$
VI	1536	5294	35967	72.3	48.7	5.83	17.11	28.9	$(PhSiO_{1.5})_{0.50}(MeSiO_{1.5})_{0.23}(Me_2ViSiO_{0.5})_{0.27}$
VII	1579	5757	39393	72.9	49.8	5.41	16.13	27.5	$(PhSiO_{1.5})_{0.53}(MeSiO_{1.5})_{0.21}(Me_2ViSiO_{0.5})_{0.26}$
VIII	1531	3671	18560	70.5	51.4	5.36	14.68	26.3	$(PhSiO_{1.5})_{0.62}(MeSiO_{1.5})_{0.12}(Me_2ViSiO_{0.5})_{0.26}$
IX	1315	3264	34567	74.9	52.5	5.21	14.39	27.2	$(PhSiO_{1.5})_{0.66}(MeSiO_{1.5})_{0.08}(Me_2ViSiO_{0.5})_{0.26}$
X	1103	3492	37673	71.9	56.8	5.56	13.35	23.5	$(PhSiO_{1.5})_{0.70}(MeSiO_{1.5})_{0.06}(Me_2ViSiO_{0.5})_{0.24}$
XI	998	4205	121662	76.6	57.5	4.98	14.81	23.7	$(PhSiO_{1.5})_{0.76}(Me_2ViSiO_{0.5})_{0.24}$

[a] TGA char yield to 1100 °C under argon. [b] The composition of example IV as determined by ^{29}Si NMR $(PhSiO_{1.5})_{0.40}(MeSiO_{1.5})_{0.39}(Me_2ViSiO_{0.5})_{0.21}$. The composition of example XI as determined by ^{29}Si NMR $(PhSiO_{1.5})_{0.75}(PhSiO(OR))_{0.01}(Me_2ViSiO_{0.5})_{0.21}$.

Table III. Analysis of Ceramic Chars Fired to 1800 °C

	char yield	elem anal. (wt %)			ceram composition (wt %)[a]		quantitative XRD	
example	(wt %)	C	O	Si	SiC	C	β-SiC	C
I	35.1	29.65	0.22	69.9	100		100	
II	41.9	32.30	0.26	67.3	96.7	3.3	100	
III	41.6	35.34	0.20	62.8	92.4	7.6	99	1
IV	44.7	38.83	0.25	57.6	87.4	12.6	99	1
V	45.8	40.30	0.26	55.5	85.3	14.7	99	1
VI	46.4	42.30	0.19	54.1	82.4	17.6	99	1
VII	47.3	43.97	0.21	51.6	80.0	20.0	99	1
VIII	47.0	45.70	0.29	49.9	77.6	22.4	98	2
IX	48.9	47.85	0.20	48.7	74.5	25.5	98	2
X	48.0	49.70	0.22	46.9	71.9	28.1	98	2
XI	48.8	52.10	0.27	44.6	68.4	31.6	97	3

[a] Based on a thermodynamic rule of mixtures calculation based on the carbon analysis.

reaction was cooled and 10 g $ViMe_2SiCl$ added. After stirring at room temperature for 2 h, the reaction was filtered through a 0.2-μm membrane and the filtrate concentrated via rotary evaporation. The resulting clear polymer was then vacuum dried for approximately 2 h at 100 °C and <1 Torr; yield 126 g; characterization given in Table II.

The desired composition, amounts of starting materials and polymer yields for all of the examples are given in Table I. The subsequent polymer characterization by gel permeation chromatography, thermal gravimetric analysis, elemental analysis, and proton magnetic resonance spectrometry is provided in Table II.

Preparation of Ceramics. Employing the following detailed procedure, the polymers described in examples I–XI were bulk pyrolyzed to ceramic materials:

Example I: $(MeSiO_{1.5})_{0.50}(PhSiO_{1.5})_{0.25}(ViMe_2SiO_{0.5})_{0.25}$. A blend of 6.55 g of the above resin and 0.06 g of Lupersol 101 (2,5-dimethyl-2,5-bis(*tert*-butylperoxy)hexane) was prepared. This blend was cross-linked at 180 °C for 1 h under argon. An aliquot of the cross-linked resin was weighed into a graphite crucible and the crucible transferred into an Astro furnace. The furnace was evacuated to <20 Torr and back-filled with argon. Under a purge of argon, the sample was heated to 1800 °C at 10 °C/min and held at temperature for 1 h before cooling to room temperature.

The corresponding char yields and compositions for the ceramics derived from the polymers described in examples I–XI are summarized in Table III.

Two polymers (examples IV and XI) were also pyrolyzed to a variety of temperatures from 1200 to 2100 °C in an effort to gain more insight into the pyrolysis chemistries of these materials over that temperature range (vide infra). The polymer samples were cross-linked and placed in the Astro furnace as described above. Pyrolysis under an argon purge was carried out at a ramp rate of 1 °C/min, to prevent overshooting of the desired temperature, with a 15-min hold at temperature before cooling to room temperature. The char yields, elemental composition and empirical formulas of the ceramics are given in Tables IV and V, respectively.

Results and Discussion

Control over the Ceramic Stoichiometry. Given the fact that high oxygen polymer systems (siloxanes) can be pyrolyzed to afford silicon carbide (eq 1), the control over the stoichiometry of the ceramic char is the key for the utility of these polymers as binders over a range of levels for the sintering of ceramic powders.

$$(RSiO_{1.5})_n \xrightarrow[1200\ °C]{} C_xSi_yO_z \xrightarrow[1800\ °C]{} ySiC + (x - y - z)C + zCO(g) \quad (1)$$

Aside from contributing SiC to the ceramic monolith these siloxane polymer binders also contribute the excess

Table IV. Analysis of Ceramic Chars from Polymer Example IV

pyrol temp (°C)	char yield (wt %)	ceram elem anal. (wt %) C	O	Si	empirical formula	quantitative XRD 3C	15R
1200	78.6	36.32	23.38	30.8	$Si_{1.0}O_{1.33}C_{2.75}$		
1300	78.6	35.00	26.12	29.5	$Si_{1.0}O_{1.55}C_{2.76}$		
1400	75.9	36.00	25.68	33.0	$Si_{1.0}O_{1.36}C_{2.55}$	trace	
1500	74.2	35.58	25.27	31.9	$Si_{1.0}O_{1.38}C_{2.60}$	trace	
1600	49.5	37.70	5.36	52.7	$Si_{1.0}O_{0.18}C_{1.67}$	90	5
1700	44.7	37.50	0.77	58.5	$Si_{1.0}O_{0.02}C_{1.50}$	95	4
1800	44.2	37.10	0.37	58.8	$Si_{1.0}O_{0.01}C_{1.47}$	97	2
1900	43.0	37.83	0.55	58.1	$Si_{1.0}O_{0.02}C_{1.52}$	96	2
2000	43.5	38.33	0.49	57.9	$Si_{1.0}O_{0.01}C_{1.54}$	96	2
2100	43.0	36.98	0.29	57.6	$Si_{1.0}O_{0.01}C_{1.49}$	96	2

Table V. Analysis of Ceramic Chars from Polymer Example XI

pyrol temp (°C)	char yield (wt %)	ceram elem anal. (wt %) C	O	Si	empirical formula	XRD 3C
1200	76.4	48.30	20.57	24.6	$Si_{1.0}O_{1.46}C_{4.58}$	
1400	75.5	50.34	20.38	25.8	$Si_{1.0}O_{1.38}C_{4.55}$	trace
1600	55.9	52.04	9.08	32.3	$Si_{1.0}O_{0.49}C_{3.75}$	85
1800	49.0	50.07	0.27	38.4	$Si_{1.0}O_{0.01}C_{3.04}$	95

carbon (optimum of 1.0–2.0 wt %) that is necessary for the sintering of SiC.[15] Previous work has shown that when excess carbon is added by a carbonaceous resin (phenolic resin or poly(methylphenylene), etc.) it is much more effective at limiting the grain growth of the silicon carbide monolith than carbon powder additions.[16]

As with silazanes the control of the carbon content in the ceramic is accomplished by controlling the chemistry of the polymer.[3,17] In general, ceramics with higher carbon levels are obtained by employing unsaturated organic groups bound to the silicon which makes them less likely to be cleaved upon pyrolysis. To establish the relationship between the amount of organic unsaturation (aryl groups) in a polymer and the amount of carbon in the ceramic, the polymers in examples I–XI were prepared and pyrolyzed to ceramics. As the mole fraction of phenyl is increased within the $(PhSiO_{1.5})_x(MeSiO_{1.5})_{0.75-x}(ViMe_2SiO_{0.5})_{0.25}$ series of siloxanes one gets increasingly higher weight percent excess carbon levels in the 1800 °C ceramics (Table III and Figure 1). *As can be seen from Figure 1, this relationship is nearly linear with a 0.997 correlation coefficient for the straight line fit.*

This control over the ceramic stoichiometry of the polymer allows for the tailoring of binders for specific forming applications while keeping the overall weight percent of excess carbon in the monolith constant. For simple die pressing or isopressing applications a polymeric binder as described in example XI, $(PhSiO_{1.5})_{0.75}(ViMe_2SiO)_{0.5})_{0.25}$ which provides 1.6 wt % excess carbon at 10% binder levels would be suitable. For more complicated forming techniques such as injection molding or extrusion where upwards of 20 wt % polymer binder is required to get sufficient flow, a binder as described in Example V $(PhSiO_{1,5})_{0,45}(MeSiO_{1,5})_{0,30}$-$(ViMe_2SiO_{0,5})_{0,25}$ that provides 1.5 wt % excess carbon at 20 wt % binder levels is appropriate. The incorporation of vinyl groups in the polymer, allows for cure of the articles once they are formed.

Conversion of Siloxanes to Silicon Carbide. Since the initial reports that siloxane resins can be used as precursors to silicon carbide ceramic powders,[8] there have been several recent literature reports that have employed a variety of techniques to characterize this low-temperature pyrolysis region.[14,18,19] Babonneau et al. has examined the pyrolysis chemistry of $(Me_2SiO)_x(SiO_2)_{1-x}$ copolymers by XRD, IR, and ^{29}Si MAS NMR spectroscopies. One of the key observations in this work is that an appreciable percentage (nearly 30% at one point) of T units are formed throughout the pyrolysis while the number of D and Q units seen by NMR fluctuate throughout the pyrolysis.[20] These T units are seen despite the fact that none are present in the starting polymers. The actual mechanism by which the T units are formed was not established and is very difficult to establish because of the polymer decomposition and volatilization of methane and hydrogen. The authors concluded that the pyrolysis from 300 to 1000 °C corresponded to the consumption of the methyl groups

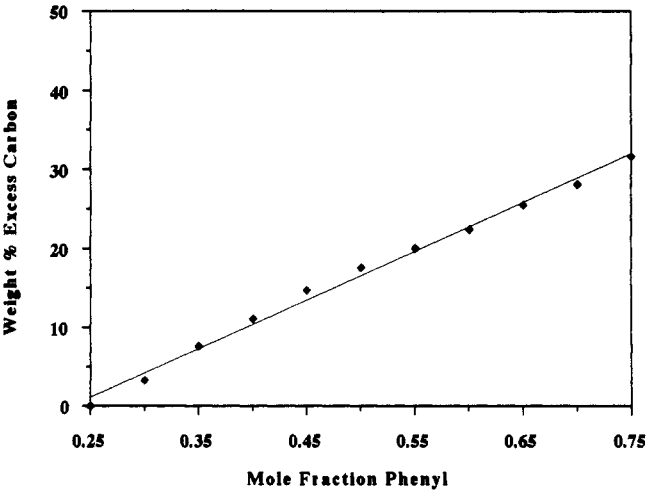

Figure 1. Weight percent excess carbon and silicon carbide obtained as a function of Phenyl content from the $(PhSiO_{1.5})_x(MeSiO_{1.5})_{0.75-x}(ViMe_2SiO_{0.5})_{0.25}$ series of siloxane polymers after pyrolysis to 1800 °C under argon.

Scheme I

$$2CH_3SiO_{1.5} \longrightarrow (CH_3)_2SiO + SiO_2$$

$$(CH_3)_2SiO + CH_3SiO_{1.5} \longrightarrow (CH_3)_3SiO_{0.5} + SiO_2$$

$$(CH_3)_3SiO_{0.5} + CH_3SiO_{1.5} \longrightarrow (CH_3)_4Si + SiO_2$$

(15) Prochazka, S. In *Ceramics for High Performance Applications*; Brook Hill: New York, 1974; pp 239–52.
(16) Prochazka, S. In *Proceedings of the Sixth Symposium on Special Ceramics*; 1974, 171–81.
(17) Burns, G. T.; Angelotti, T. P.; Hanneman, L. F.; Chandra, G.; Moore, J. A. *J. Mater. Sci.* **1987**, *22*, 2609–14.
(18) Belot, V.; Corriu, R. P. J.; Leclercq, D.; Mutin, P. H.; Vioux, A. *J. Mater. Sci. Lett.* **1990**, *9*, 1052–4.
(19) Laine, R. M.; Rahn, J. A.; Youngdahl, K. A.; Babonneau, F.; Hoppe, M. L.; Zahng, Z. F.; Harrod, J. F. *Chem. Mater.* **1990**, *2*, 464–72.
(20) Conventional designations for the structural units or coordination spheres about the silicon in siloxane polymers are as follows: C–SiC_4; M–$SiOC_3$; D–SiO_2C_2; T–SiO_3C; Q–SiO_4.

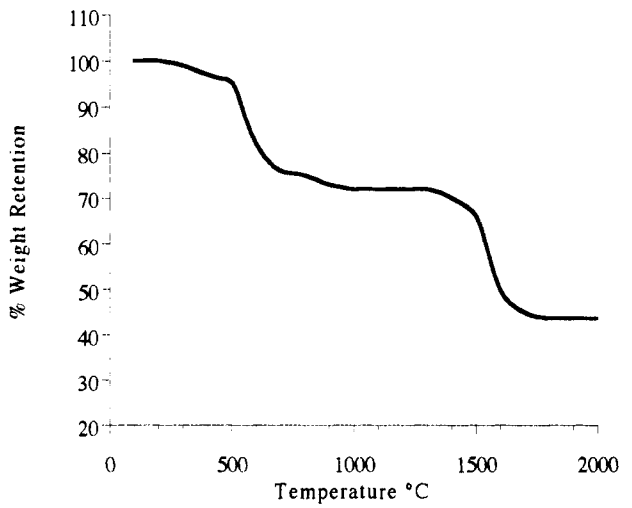

Figure 2. TGA curve to 2000 °C for the siloxane polymer from example IV, $(PhSiO_{1.5})_{0.40}(MeSiO_{1.5})_{0.35}(ViMe_2SiO_{0.5})_{0.25}$. This composite curve was developed from a TGA experiment to 1200 °C and bulk pyrolysis to 2100 °C.

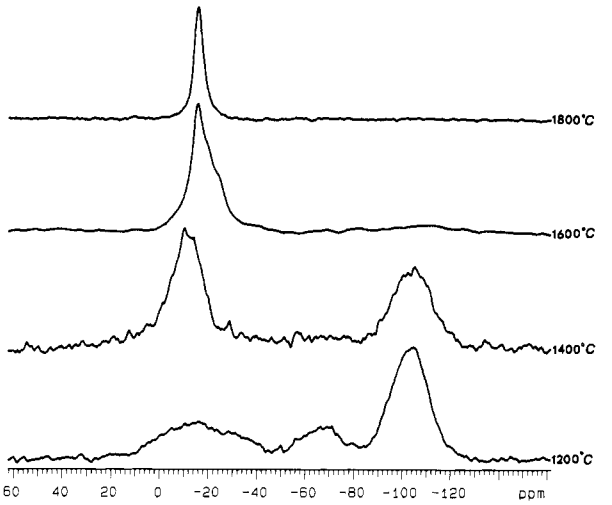

Figure 3. Solid-state ^{29}Si MAS NMR spectra of the ceramic chars derived from $(PhSiO_{1.5})_{0.40}MeSiO_{1.5})_{0.35}(ViMe_2SiO_{0.5})_{0.25}$ (example IV) at 1200, 1400, 1600, and 1800 °C.

which results in the conversion of the D into T and then Q units.

Corriu et al. has studied the pyrolysis chemistries of three siloxane systems $HSiO_{1.5}$, $(MeSiO_{1.5})_{0.50}(Me_2SiO)_{0.50}$ and $MeSiO_{1.5}$.[18,21] In these papers the authors identified, by ^{29}Si CP/MAS NMR, the formation of D and Q units, after pyrolysis to temperatures of 600 °C, from all T starting materials (both $HSiO_{1.5}$ and $MeSiO_{1.5}$). From the T, D polymer system ($(MeSiO_{1.5})_{0.50}(Me_2SiO)_{0.50}$), the authors report the presence of M, D, T, and Q units by ^{29}Si CP/MAS NMR after pyrolysis to 600 °C. Corriu suggests that these results support the occurrence of a redistribution reaction involving Si–C and Si–O bonds as shown in Scheme I. The authors admit that this redistribution chemistry is really more complicated than the above reactions indicate since at the temperatures where these reactions are seen (600 °C) other concomitant reactions occur to account for the loss of methane and hydrogen from the system.[21]

The general pathway in which the siloxane polymers we have studied thermally decompose into silicon carbide ceramics can be seen from a TGA curve of the polymer $(PhSiO_{1.5})_{0.40}(MeSiO_{1.5})_{0.35}(ViMe_2SiO_{0.5})_{0.25}$ (example IV) shown in Figure 2. The pyrolysis occurs in two regions: (1) a low-temperature region that involves the loss of organic materials to ~1200 °C (TGA MS analysis of these materials has identified benzene, ethylene, and acetylene as the predominant volatiles at 550 °C while methane is evolved from 650 to 875 °C) and (2) a high-temperature region that converts the SiCO inorganic material to a SiC ceramic (above 1400 °C).

These siloxane polymers consistently have char yields of 45–48 wt %, when there is sufficient excess carbon present within the material to allow for efficient carbothermic reduction of the high oxygen polymer (examples IV–XI). In cases where the amount of excess carbon is below 10 wt % a lower overall char yield results (examples I–III). We believe that these lower char yields are due to inefficient carbothermic reduction when lower levels of excess carbon are present and hence evolution of SiO, which is a key intermediate in the reduction of SiO_2 with carbon (vide infra). This is supported by the similar 1000 °C TGA char yields (Table II) seen for all of the polymers regardless of the levels of excess carbon.

Elemental and X-ray Diffraction Analysis. Previous work describes the "redistribution" chemistry associated with the pyrolysis of siloxane polymers and silsesquioxane gels to temperatures sufficient to make SiCO inorganic materials.[14,18,19,21] To understand the transformation of these SiCO inorganic materials to silicon carbide, the pyrolysis of $(PhSiO_{1.5})_{0.40}(MeSiO_{1.5})_{0.35}(ViMe_2SiO_{0.5})_{0.25}$ (example IV, a polymer that affords a small amount of excess carbon) was examined. Samples of polymer were heated as described previously from 1200 to 2100 °C. The pyrolysis was stopped at 100 °C intervals, and the residue analyzed. The overall char yields, total elemental analysis, and quantitative X-ray diffraction analysis are presented in Table IV.

From examination of the char yields and the elemental analysis, it appears that the 1200 °C SiCO inorganic material is compositionally stable to 1500 °C. By 1600 °C the material decomposes with the evolution of CO.[22] By 1800 °C only trace levels of oxygen remain in the system and a compositionally stable SiC material formed. Concomitant with the loss of the oxygen from the system, is identification of substantial amounts of crystalline β-SiC by XRD (Table IV). To examine the effect of the amount of excess carbon on the carbothermic reduction of these systems, a similar set of experiments was carried out on $(PhSiO_{1.5})_{0.75}(ViMe_2SiO_{0.5})_{0.25}$ (example XI, the polymer that affords the greatest amount of excess carbon within this series). The char chemistry of this polymer was examined at 1200, 1400, 1600, and 1800 °C. A summary of the char yields, elemental and XRD analyses is in Table V. Additional excess carbon does not change this decomposition since substantial oxygen levels remain even after pyrolysis to 1600 °C and no appreciable amounts of crystalline SiC are seen by XRD until 1600 °C.

Despite the lack of any substantial compositional changes in the chars between 1200 and 1500 °C, the X-ray diffraction analyses indicate that structurally some changes in the materials are taking place (Table IV first four entries, Table V first two entries). To better understand the transformation from amorphous to crystalline ceramics,

(21) Belot, V.; Corriu, R.; Leclercq, D.; Mutin, P. H.; Vioux, A. *Chem. Mater.* **1991**, *3*, 127–31.

(22) The pyrolysis conditions (furnace construction, placement of sample within, ramp rate, gas flow rate) along with the sample being pyrolyzed (geometry especially the surface area to volume relationship, i.e., bulk polymer versus fiber pyrolysis) play important rolls in determining the onset of carbothermic reduction along with the relative ratios of CO and SiO being evolved.

we turned to other analytical techniques.

^{29}Si MAS NMR Analysis. To probe the structural changes taking place from 1200 to 1400 °C and those that take place during the carbothermic reduction to 1800 °C, we carried out a series of ^{29}Si MAS NMR experiments on the ceramics derived from the polymer from example IV. Figure 3 shows the results of these experiments. At 1200 °C the spectral features associated with all the possible tetrahedral structures SiC_4 (δ = −18.3), SiC_3O (δ = +6.7), SiC_2O_2 (δ = −22.1), $SiCO_3$ (δ = −65.0), and SiO_4 (δ = −107) are seen.[23,24] Of these, the SiO_4 resonance centered at −105 ppm was the most distinct. By simulating this spectrum with individual components, a stoichiometry of $(SiC_4)_{0.11}(SiC_3O)_{0.14}(SiC_2O_2)_{0.09}$ $(SiCO_3)_{0.17}(SiO_4)_{0.49}$ was obtained for the silicon species present. The overall stoichiometry by ^{29}Si MAS NMR was $Si_{1.0}O_{1.4}C_x$ which is in good agreement with the elemental analysis of the ceramic char (first entry in Table II).[25] The presence of all the possible tetrahedral structures (Q, T, D, M, and C) in the 1200 °C ceramic residue from a polymer that only contained M and T structural units was surprising. Obviously the "redistribution" chemistry discussed by Corriu in the pyrolysis of methylsilsesquioxane occurs in other silicone resins regardless of their original structure and amount of carbon present in the system.

The ^{29}Si MAS NMR spectrum obtained from the 1400 °C ceramic sample shows two very distinct resonances centered at −105 and −12 ppm. These resonances correspond approximately to those for SiO_4 and SiC_4, respectively. Therefore, even though the material appears to be compositionally stable, structural changes have taken place. Although, no further weight loss was seen there was some evidence of structural changes from the trace amount of β-SiC seen by X-ray diffraction (vide supra). *The XRD results in combination with this NMR characterization indicate that substantial amounts of β-SiC are formed at 1400 °C, not by carbothermic reduction process but by a continuation of the C for O redistribution chemistry discussed by Corriu.* In this case this redistribution chemistry is even more clear cut since no weight loss is seen between 1200 and 1400 °C. The amount of SiC formed by this redistribution chemistry is controlled by the relative amounts of carbon and oxygen present in the ceramic.

After pyrolysis to 1600 °C the ^{29}Si MAS NMR spectrum of the resulting ceramic now is comprised of a strong, nearly single peak centered at −16 ppm and a very broad resonance at −115 ppm corresponding to SiC_4 and SiO_4 environments respectively. This SiC_4 resonance is broadened compared to commercial crystalline β-SiC,[26] which indicates that there are a wide range of SiC_4 environments in this material. This is consistent with ^{29}Si MAS NMR spectra of amorphous silicon carbide materials and the fact that the silicon carbide in this sample was derived from an amorphous precursor.[27] The peak maxima is in the same chemical shift range of crystalline silicon carbide polytypes, consistent with the typical silicon environments being not much different from those found in

Scheme II

$$SiO_2(s) + CO(g) \longrightarrow SiO(g) + CO_2(g)$$

$$CO_2(g) + C(s) \longrightarrow 2CO(g)$$

$$SiO(g) + 2C(s) \longrightarrow SiC(s) + CO(g)$$

$$SiO_2(s) + 3C(s) \longrightarrow SiC(s) + 2CO(g)$$

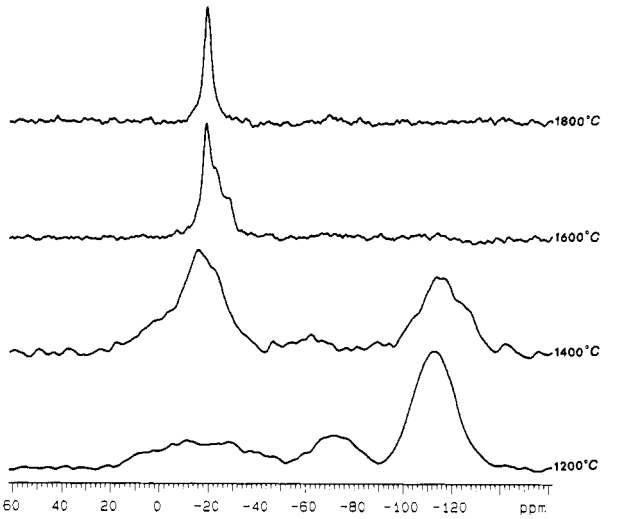

Figure 4. Solid-state ^{29}Si MAS NMR spectra of the ceramic chars derived from $(PhSiO_{1.5})_{0.75}(ViMe_2SiO_{0.5})_{0.25}$ (example XI) at 1200, 1400, 1600, and 1800 °C.

100% crystalline forms.[26] The TEM characterization (vide infra) provide no evidence for other polytypes of silicon carbide only β-SiC being present in the system. In addition, there is a measurable weight loss and changes in the elemental analysis of the chars. The ceramic composition data shows only a fraction of the original level of oxygen present in the polymer remains (5.36 compared to 17.52 wt %). The XRD data also shows substantial amounts of crystalline SiC present (Table II). *This ceramic material has now seen temperatures above 1400 °C which are sufficient to begin the carbothermic reduction process that is responsible for the large increase in intensity of the SiC_4 resonance.*[22]

After pyrolysis to 1800 °C the only species present by ^{29}Si MAS NMR was the SiC_4 resonance centered at −16 ppm. This is consistent with the negligible levels of oxygen found in the ceramic char and the high amounts of crystalline SiC by XRD measurements.

The absence of evidence for any mixed silicon oxycarbides in the ^{29}Si MAS NMR analysis agrees with kinetic data that the carbothermic reduction proceeds by the formation of SiO and CO_2 as key vapor phase *intermediates* (Scheme II).[28-30] If there were no vapor-phase mechanism to explain this carbothermic reduction, one would expect to find evidence for the mixed silicon oxycarbides which would be the necessary intermediates of a solid-state reaction mechanism.

A similar set of ^{29}Si MAS NMR experiments were carried out on $(PhSiO_{1.5})_{0.75}(ViMe_2SiO_{0.5})_{0.25}$ (example XI, the polymer that afforded the greatest amount of excess carbon within this series). Figure 4 shows the results of these experiments. As with the lower carbon system, the ma-

(23) (a) Taylor, R. B.; Parbhoo, B.; Fillmore, D. M. In *The Analytical Chemistry of Silicones*; John Wiley and Sons: New York, 1991. (b) Marmmann, H. In *NMR Basic Principles and Progress*; Springer-Verlang: London, 1981; pp 65–235.

(24) Guth, J. R.; Petuskey, W. T. *J. Phys. Chem.* **1987**, *91*, 5361–4.

(25) The relative amount of carbon present cannot be quantified since the NMR experiment describes only the immediate bonding arrangement about the silicon and a majority of the carbon in this system is not directly bound to the silicon.

(26) Apperley, D. A.; Harris, R. K.; Marshall, G. L.; Thompson, D. P. *J. Am. Ceram. Soc.* **1991**, *74*, 777–82.

(27) Hartman, J. S.; Richardson, M. F.; Sheriff, B. L.; Winsborrow, B. G. *J. Am. Chem. Soc.* **1987**, *109*, 6059–67.

(28) Klinger, N.; Strauss, E. L.; Komarek, K. L. *J. Am. Ceram. Soc.* **1966**, *49*, 369–75.

(29) Pultz, W. W.; Hertl, W. *Trans. Faraday Soc.* **1966**, *62*, 2499–504.

(30) Miller, P. D.; Lee, J. G.; Cutler, I. B. *J. Am. Ceram. Soc.* **1979**, *62*, 147–9.

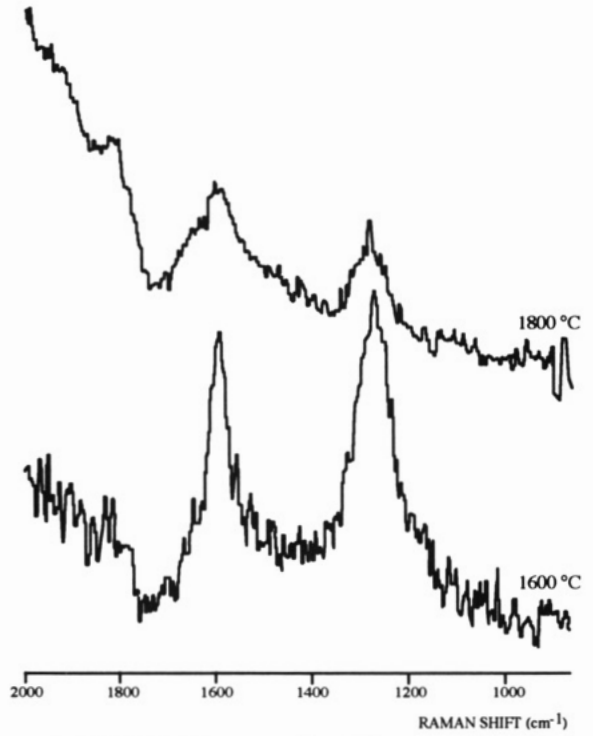

Figure 5. Solid-state Raman spectra of the ceramic chars derived from $(PhSiO_{1.5})_{0.40}(MeSiO_{1.5})_{0.35}(ViMe_2SiO_{0.5})_{0.25}$ (example IV) at 1600 and 1800 °C.

terial is a complicated mixture of all the SiCO tetrahedra possible at 1200 °C. This mixture of materials then moves to the two most thermodynamically favored materials being SiO_4 and SiC_4 at 1400 °C. The carbothermic reduction of the SiO_4 to SiC_4 is nearly complete by 1600 °C and a very sharp resonance that corresponds to SiC_4 is the only one seen at 1800 °C. In general, the higher level of carbon in this system did not drastically affect the high-temperature redistribution chemistry followed by carbothermic reduction.

Raman Analysis. While the ^{29}Si MAS NMR experiments provided insights into the chemistries associated with silicon in the conversion of these polymers to ceramics, they provided no information into the nature of the carbon not bound to the silicon. In an effort to characterize the free or excess carbon in the 1400, 1600 and 1800 °C ceramic chars from $(PhSiO_{1.5})_{0.40}(MeSiO_{1.5})_{0.35}(ViMe_2SiO_{0.5})_{0.25}$ (example IV, a polymer that affords a small amount of excess carbon), we turned to Raman spectroscopy. Raman spectroscopy has become one of the preferred tools for the characterization of disordered polycrystalline and non crystalline graphitic carbons.[31] The spectra are shown in Figure 5.

No Raman bands of any intensity are seen in the spectra of the 1400 °C ceramic char. In contrast the spectra of the 1600 and 1800 °C materials are dominated by two bands centered at 1270 and 1590 Raman wavenumbers (cm^{-1}).[32] These two bands are diagnostic for the D and G bands of graphitic carbon respectively. Along with verification that graphitic type carbons exist in these samples some information is gained about the domain size and the relative order or disorder of the graphitic carbon. The relative domain size correlates inversely with the intensity ratio of the D to G band (I_D/I_G), while the band

(31) Knight, D. S.; White, W. B. *J. Mater. Res.* **1989**, *4*, 385–93 and references therein.

(32) The Raman spectrum of the 1400 °C sample showed no bands above the scatter of the baseline.

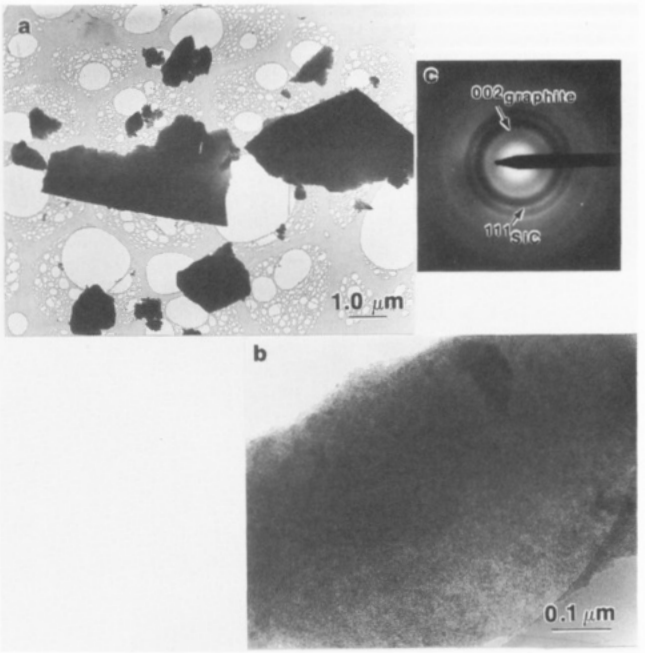

Figure 6. Low- and medium-magnification TEM images of the 1400 °C ceramic (a) and (b) along with the SADP (c) indicating the presence of both graphite and silicon carbide.

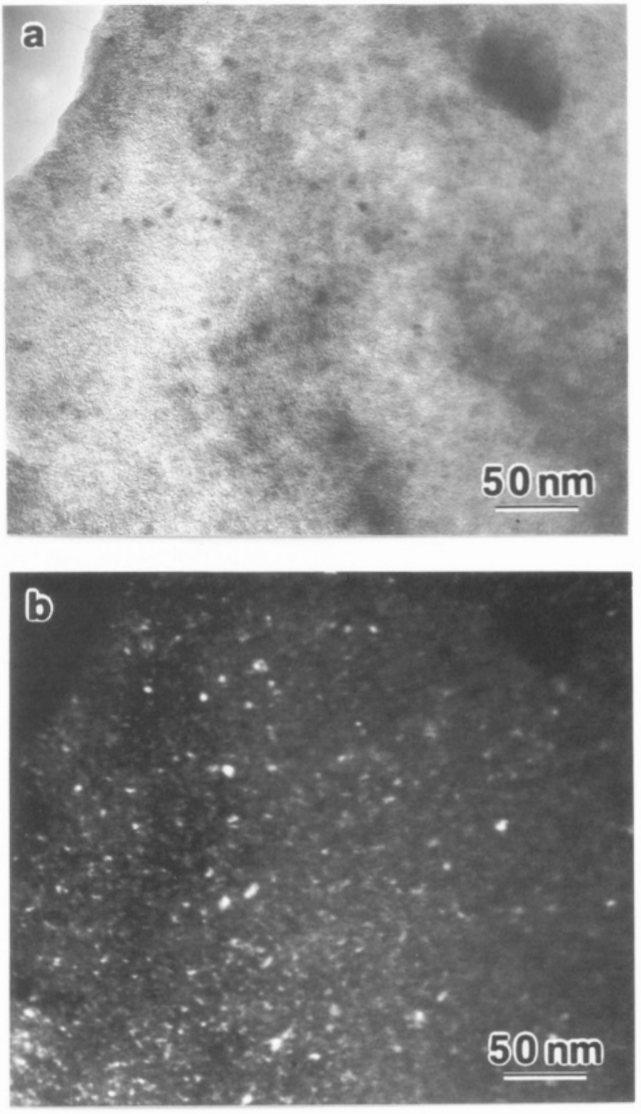

Figure 7. Bright field (a) and dark field (b) TEM images of the 1400 °C ceramic.

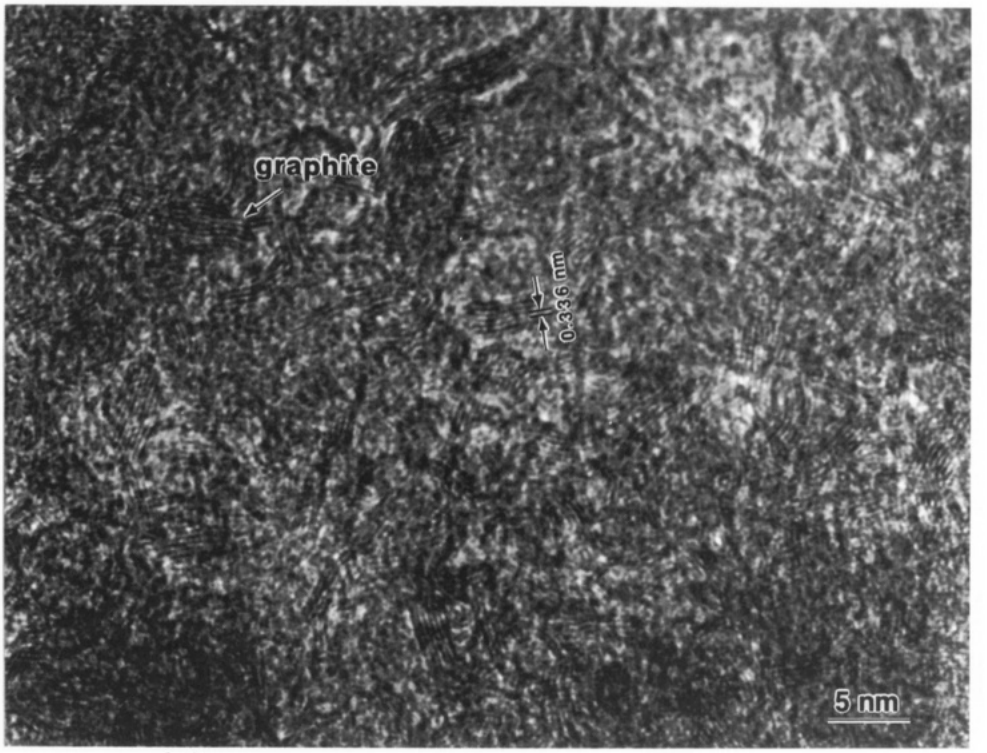

Figure 8. High-resolution micrograph displaying the graphite lattice fringes in the 1400 °C ceramic sample.

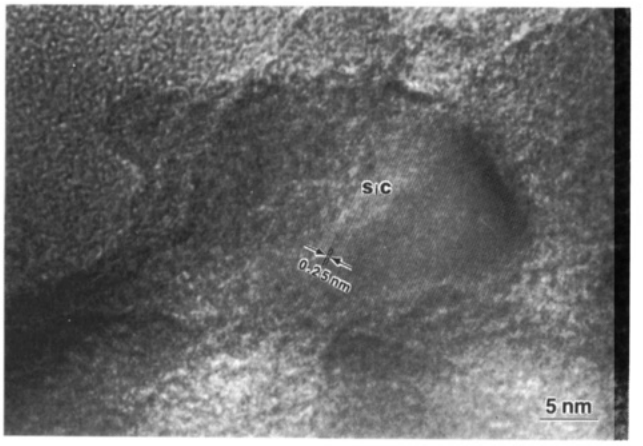

Figure 9. Lattice fringes of a silicon carbide crystallite imaged in the 1400 °C ceramic sample.

width of the G band relates to the disorder within the carbon sheets.[33,34]

For the 1600 °C sample the D to G intensity ratio is 1.2 and the G band bandwidth is 56 cm^{-1}. This corresponds to an average domain size of ~35 Å and a disordering similar to that of a glassy carbon.[31] For the 1800 °C sample the intensity ratio is 0.9 and the G band bandwidths is 110 cm^{-1}. This corresponds to an average domain size of ~50 Å and an ordering similar to that of a high hydrogen diamond film or a burnt wood.[31] Both the I_D/I_G intensity ratio and the width of the G band appear to be independent variables that characterize the Raman spectra of graphitic materials. It would appear from this analysis that the graphitic carbon (1) increases its domain size but (2) becomes more disordered upon pyrolysis from 1600 to 1800 °C. We believe that this increased disorder is related to the nature of the turbostratic graphite as seen by TEM analysis (vide infra).

(33) Tuinstra, R.; Koening, J. L. *J. Chem. Phys.* **1970**, *53*, 1126.
(34) Lespade, P.; Marchand, A.; Couzi, M.; Cruge, F. *Carbon* **1984**, *22*, 375.

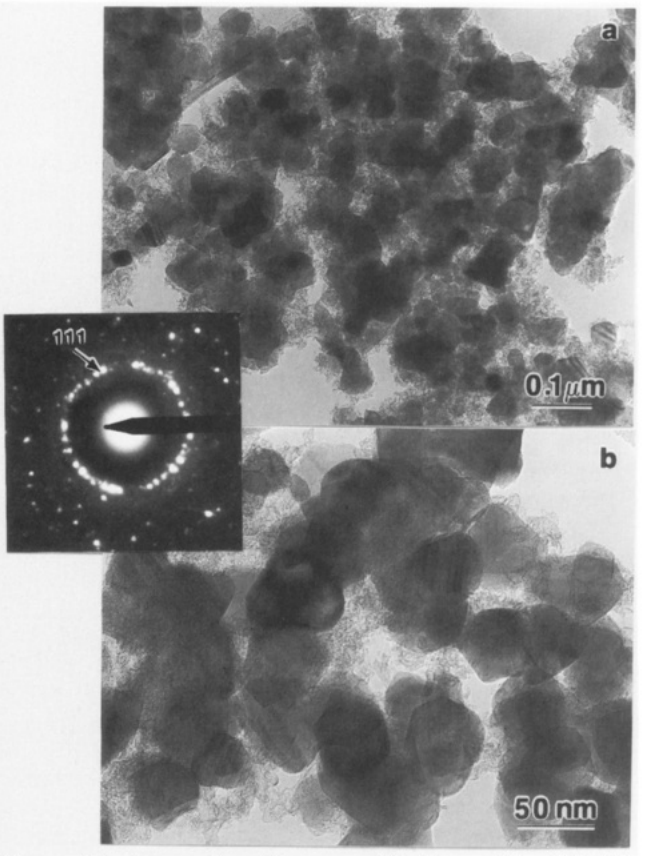

Figure 10. Low and medium magnifications of the 1600 °C ceramic a and b and the SADP (inset) indicating the presence of both graphite and silicon carbide.

Transmission Electron Microscopy Analysis. For a complete characterization of the microstructure of these ceramic samples, we turned to conventional and high-resolution transmission electron microscopy. The samples examined are the same 1400, 1600, and 1800 °C ceramic chars from $(PhSiO_{1.5})_{0.40}(MeSiO_{1.5})_{0.35}(ViMe_2SiO_{0.5})_{0.25}$

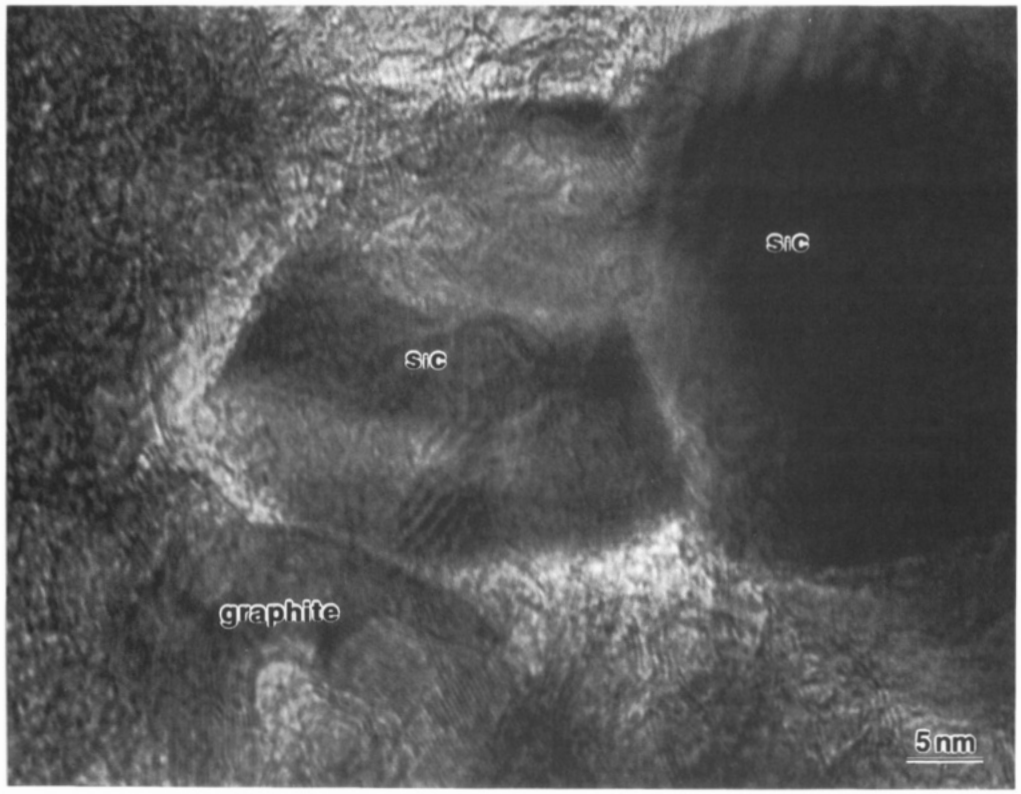

Figure 11. High-resolution lattice images of the graphite and moiré fringes from overlapping silicon carbide crystallites, also visible in the 1600 °C ceramic sample.

(example IV) that we had examined by the previously discussed techniques. Electron micrographs from these TEM examinations are shown in Figures 6–13.

Electron microscopy images from the 1400 °C ceramic are shown in Figures 6–10. The low and medium magnifications of the ceramic particles shown in Figure 6 demonstrate that the particles are large enough to study the various phases, their relative distribution, and size. Also shown in Figure 6 is a selected area diffraction pattern (SADP). The inner ring corresponds to graphite (0.336 nm), and the second ring corresponds to (111) β-SiC.[35] Figure 7 shows a bright- and dark-field set of images with the dark-field image obtained from a portion of the first SiC ring. Within the dark-field image it is apparent that the bulk of the SiC crystals (bright spots) are less than 10 nm in size. Many of the areas contained less SiC which indicates that the distribution of the β-SiC is not homogeneous at this temperature.[36] Figure 8 is a high-resolution micrograph displaying graphite lattice fringe images. The areas between the groups of fringes were not directly identified but likely contain amorphous SiO_2 and SiC crystallites. There was no apparent SiC in the area imaged in Figure 8 but an ~5-nm SiC crystallite imbedded in a powder particle that is roughly 50 nm thick would be difficult to image. Some of the larger SiC crystallites were imaged as is shown in Figure 9. One good size crystallite is shown in the center of this image while another can be seen in the upper right corner.

Figures 10 and 11 are transmission electron micrographs of the 1600 °C ceramic char. The ~50-nm particles shown in Figure 10a,b are β-SiC (now an order of magnitude larger than in the 1400 °C char). Some evidence of twinning in the crystallites is seen. The strong spotted diffraction ring in the SADP is (111) SiC with the barely visible inner ring belonging to the weakened graphite diffraction pattern. Figure 11 shows clear evidence of both the graphite and the silicon carbide crystallites in the same imaging area. The lattice fringes are generally not visible in the SiC; the widely spaced lines are moiré patterns, resulting from overlaps of SiC crystallites.

TEM images of the 1800 °C ceramic are shown in Figures 12 and 13. The now large silicon carbide crystallites (~100 nm) are clearly visible in Figure 12a, with most of the crystallites twinned as in Figure 12b. In Figure 13 the two-dimensional structure of the twinned SiC is visible (at the bottom of the micrograph) along with typical "turbostratic" graphite.[37] This very tortured turbostratic graphitic structure is likely responsible for the high degree of disorder seen by Raman spectroscopy.

Summary. The observations that have been made through the combination of analytical techniques employed on ceramics derived from siloxane polymers are summarized below.

1200 °C. The material is an SiCO amorphous ceramic that is obtained in ~75 wt % char yield. The silicon environments are best described as mixtures of SiC_4, SiC_3O, SiC_2O_2, $SiCO_3$, and SiO_2 as observed by ^{29}Si MAS NMR with SiO_4 being the predominant environment. No information can be given on the nature of the carbon not bound to the silicon.

1400 °C. No further weight loss is seen from the 1200 °C ceramic (char yield is still ~75 wt %) and no bulk compositional change, but trace amounts of β-SiC are seen by X-ray diffraction. ^{29}Si MAS NMR shows dramatic structural changes from the 1200 °C sample with nearly

(35) Note that some areas of this sample showed much weaker SiC rings.

(36) Since only a portion of the diffraction ring is used for imaging, the dark-field image shows only a portion of the SiC crystallites in the area.

(37) Note, it is likely that this very tortuous turbostratic graphite structure is responsible for the higher "disorder" of the graphite seen in the Raman spectroscopy of this ceramic.

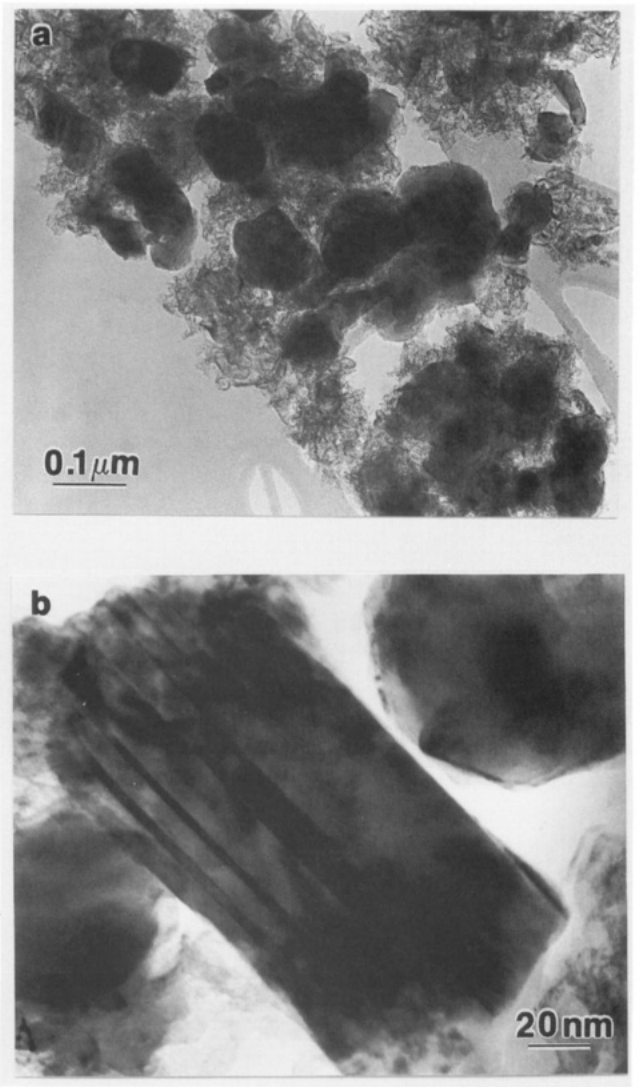

Figure 12. Micrographs indicative of the nature of the 1800 °C pyrolyzed sample (a) and depicting a twinned SiC crystal (b).

exclusive SiC_4 and SiO_4 environments (an Si–O for SiC redistribution). By TEM analysis the crystalline β-SiC domains are ~5 nm in size. By Raman spectroscopy no further information is obtained about the carbon not bound to the silicon. TEM analysis showed the presence of very finely divided graphitic domains that are less than 5 nm in size.

1600 °C. The char yield has now dropped to ~50 wt % with substantial amounts of oxygen (~80% of that present at 1200 °C) having been lost by carbothermic reduction and measurable amounts of crystalline β-SiC seen by XRD. The ^{29}Si MAS NMR spectrum shows nearly all of the silicon as SiC_4 with only trace amounts present as SiO_4. The domain size of the β-SiC crystallites is ~50 nm by TEM analysis. Raman spectroscopy gives us information for the first time that the excess carbon is similar to a highly disordered glassy carbon with a domain size of ~35 Å. The graphite seen by TEM is now much more organized into larger domains although its quantity is decreased, as evidenced from the weakened graphite diffraction ring.

1800 °C. Carbothermic reduction is complete. The overall char yield is ~45 wt %, and the sample is a crystalline mixture of α- and β-SiC by XRD analysis. The ^{29}Si MAS NMR spectrum shows a very sharp resonance for SiC_4 and no other silicon environments. The TEM analysis shows very large (~100 nm) β-SiC crystallites with the majority of them twinned. Distinct α-SiC was not observed by TEM, and it appears that the α reflections in the XRD resulted from stacking faults in the β structure. The Raman spectrum indicates that the excess carbon is quite disordered, like that of a poorly crystalline diamond carbon, with a domain size of ~50 Å. By TEM the graphitic carbon has a structure that is typical of turbostratic graphite.

Conclusions

The preparation of siloxane polymers and their conversion to silicon carbide was investigated. These polymers are useful as binder materials for ceramic powders in the preparation of dense (sintered) ceramic monoliths. The chemistry of the polymers can be altered to control the stoichiometry of the ceramic, thereby making them useful over a range of polymer binder levels. The ability to cure these ceramic binders imparts a strength for handling, machining, etc., that is substantially higher than what is seen with conventional binder technologies. Insights into

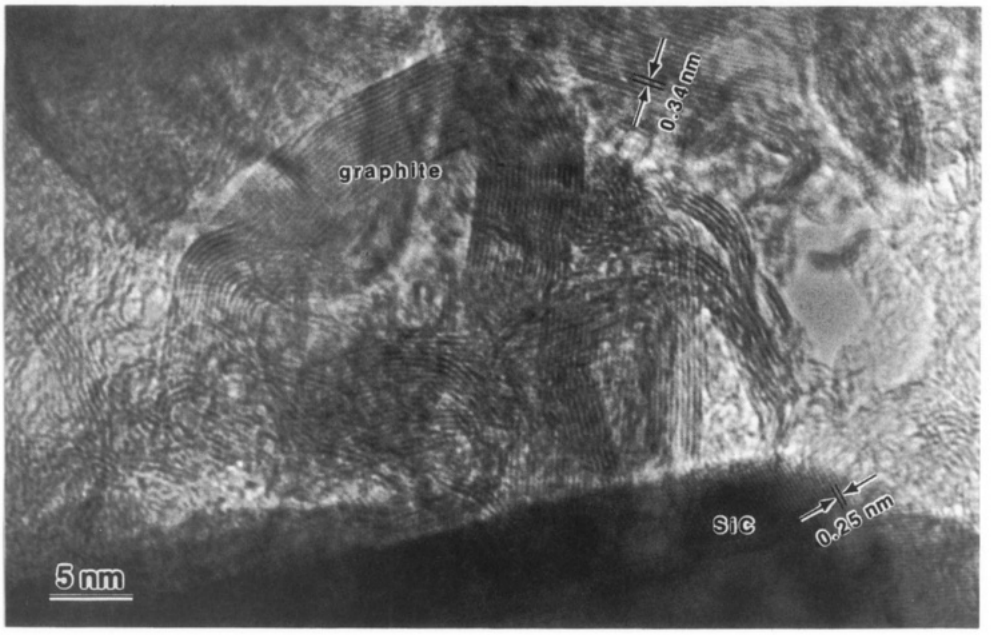

Figure 13. Identification of both twinned silicon carbide and graphite in the 1800 °C sample.

the conversion of these high-oxygen polymers to low-oxygen silicon carbide ceramics were obtained by analyzing the pyrolysis products by elemental analysis, quantitative X-ray diffraction, ^{29}Si MAS NMR spectroscopy, Raman spectroscopy, and transmission electron microscopy. We have found that the pyrolysis proceeds by the formation of an amorphous SiCO material at 1200 °C, that is composed of all possible SiCO coordination tetrahedra. Surprisingly this ceramic material is compositionally stable to ~1500 °C. At 1400 °C this material has structurally undergone a Si–O for Si–C redistribution into SiC_4 and SiO_4 as the silicon environments. The carbon not bound to the silicon is present as small (~5 nm) discrete domains of graphite. After pyrolysis to 1600 °C the ceramic loses ~80% of the oxygen present at 1200 °C and is composed predominantly of crystalline β-SiC with only traces of SiO_4. The excess carbon present is similar to a glassy carbon with ~35-Å domain size. The lack of any evidence for mixed SiCO species at these temperatures supports a vapor-phase carbothermic reduction mechanism as described in Scheme II, with SiO and CO_2 as the key intermediates. At 1800 °C the pyrolysis is complete, and the final ceramic is composed of substantial amounts of SiC with many of the SiC crystallites twinned. The carbon is a disordered diamond type of carbon with a ~50-Å domain size and a structure typical of turbostratic graphite.

Acknowledgment. The authors thank Dow Corning Corp. for the support of this work and Dr. Ann Leugers of the Dow Chemical Co. for her assistance with the Raman spectroscopy. Microstructural analysis was done at the Center for Microanalysis of Materials of the Materials Research Laboratory, UIUC, which is supported by the U.S. Department of Energy under Contract DE-FG02-91ER45439.

Registry No. SiC, 409-21-2.

Spectroscopic Characterization of Rare-Earth Octa-*tert*-butylbisphthalocyanine Complexes

D. Battisti, L. Tomilova, and R. Aroca*

Materials and Surface Science Group, Department of Chemistry and Biochemistry, University of Windsor, Windsor, Ontario, Canada N9B 3P4

Received June 15, 1992. Revised Manuscript Received September 24, 1992

The spectroscopic characterization of rare-earth octa-*tert*-butylbisphthalocyanine (R_8Pc_2Ln or $LnPc^t_2$) complexes is reported. Surface-enhanced resonance Raman of Langmuir–Blodgett films on Au island films, infrared of solids and UV–visible spectra of solid films and solutions were recorded. Complementary spectroscopy data on ultrathin solid films of rare-earth-unsubstituted bisphthalocyanines ($LnPc_2$) were also obtained. The complexes that were studied were the blue and the green materials of lanthanide (Ln) elements that were obtained by direct synthesis. The green material previously assigned to the stable free radical in the $LnPc_2$ series, gave characteristic electronic, infrared, and resonant Raman spectra for the entire $LnPc^t_2$ series. The blue material $LnHPc^t_2$ (and $LnHPc_2$) produced infrared, Raman, and electronic spectra that could be associated with the presence of two Pc^{2-} ligands. The spectral properties of the blue form were similar to that of $ZrPc_2$ where the central atom Zr(IV) is attached to two Pc^{2-} ligands. The synthesis of lanthanide mono and bisphthalocyanines are also described.

Introduction

The changes in the optical spectra of liquids and solids by the presence of an external electric field was referred to as the "electrochromic" effect. The term was introduced by Platt[1] for an effect that was mostly observed in aromatic compounds.[2] The electrochromic effect is commonly invoked to describe the faradaic electrochemical reaction that results in a color change of a material deposited on the surface of an electrode.[3,4] The electrochromic properties of rare-earth element (REE) bisphthalocyanines have stimulated a thorough investigation of these compounds.[5] The materials could also find potential applications in such areas as gas sensors and molecular electronics.[6,7]

Metal-free phthalocyanine H_2Pc and metalated phthalocyanine MPc that are composed of a single Pc ligand are blue. Their absorption spectra are dominated by a Soret and a Q band. However, transition-metal complexes consisting of a single Pc ligand may show an additional absorption band in the 500-nm region (assigned to a charge-transfer transition), and they appear green. An extensive discussion on the electronic properties of Pc molecules can be found in a recent review by Stillman and Nyokong.[7] Mono Pc of rare-earth metals (i.e., $LnPc^tX$, Pc^t = tetra-*tert*-butylphthalocyanine, X = anion)[8] are also characterized by a simple absorption spectrum without the charge-transfer band in the 500-nm region. The one-electron oxidation product of $LnPc^tX$, however, contained an absorption band in the 500-nm region. Under mild oxidative conditions, the oxidation of the Ln^{3+} cation can be ruled out, and the observed absorption band near 500

* To whom correspondence should be directed.

(1) Platt, J. R. *J. Chem. Phys.* **1961**, *34*, 862.
(2) Labhart, H. *Adv. Chem. Phys.* **1967**, *13*, 179.
(3) Collins, G. C. S.; Schiffrin, D. J. *J. Electroanal. Chem.* **1982**, *139*, 334.
(4) Corker, G. A.; Grant, B.; Clecak, N. J. *J. Electrochem. Soc.* **1979**, *126*, 1339.
(5) Liu, Y.; Shigehara, K.; Hara, M.; Yamada, A. *J. Am. Chem. Soc.* **1991**, *113*, 440.
(6) Battisti, D.; Aroca, R. *J. Am. Chem. Soc.* **1992**, *114*, 1201.
(7) *Phthalocyanines Properties and Applications*; Leznoff, C. C., Lever, A. B. P., Eds.; VCH Publishers: New York, 1989.
(8) Subbotin, N. B.; Tomilova, L. G.; Kostromina, K. A.; Luk'yanets, E. A. *Zh. Obshch. Khim.* **1987**, *56*, 345.

0897-4756/92/2804-1323$03.00/0